

Numerical study of the effect of geometry and operating parameters on the performance of Savonius vertical axis wind turbine

J. Ramarajan and S. Jayavel*

Department of Mechanical Engineering, Indian Institute of Information Technology, Design and Manufacturing, Kancheepuram, Chennai 600 127, India

The Savonius turbine is a vertical axis wind turbine (VAWT) suitable to be mounted on rooftops of high-rise buildings. It is a viable technology for power generation. The operating parameters and rotor design have a significant effect on the performance of VAWT. We have studied the effects of various parameters such as number of blades, blade arc angle, overlap ratio and gap width ratio on the performance of VAWT. Data from the literature have been reviewed for completeness. Two-dimensional numerical study subjected to a thorough grid independence study was conducted using ANSYS Fluent 15.0, and the results have been validated. The results show that the rotor system with two-blade arrangement performs better at tip speed ratio of 0.8. The rotor with gap width ratio of 0.15 and blade arc angle of 180° was found to perform better at a wind velocity of 7 m/s. Overlap ratio and modifications in the blade were found to have a negative effect on the performance.

Keywords: Numerical study, power generation, rotor design, rooftop systems, tip speed ratio, wind turbine.

POPULATION growth and industrial modernization have led to an exponential increase in energy consumption. Use of fossil fuels and the resulting emissions have forced us to explore other clean and renewable sources of energy. Born *et al.*¹ discussed the importance of renewable energy resources and analysed possible combinations of renewable energy technologies among available renewable energy sources. Wind is one of the best clean and renewable sources of energy available day and night. Research on wind turbines is currently active and new methods to improve conversion efficiency are evolving. Wind turbines are classified with respect to position of shaft as horizontal axis wind turbines (HAWTs) and vertical axis wind turbines (VAWTs). The blades of HAWT are perpendicular to the wind direction and receive power for the entire cycle. HAWTs are generally installed at high altitudes for more power production. An increase in altitude by 10 m leads to 30% increase in efficiency;

this is due to increase in air flow by 20% (ref. 2). However, installing HAWTs at higher altitudes requires high installation and maintenance cost.

VAWTs are classified into Savonius and Darrieus according to the type of force acting on turbine blades. In Darrieus type VAWT, lift and drag forces are involved, whereas in Savonius type VAWT, drag force alone is involved in rotating the turbine. Therefore, design of blades for Savonius turbine is simple. The turbine was originally developed and patented by Savonius in the 1920s³⁻⁵. Later, Savonius used it for pumping liquids⁴. The main advantages of Savonius turbines are that they do not require a yaw system, i.e. the turbine is independent of wind direction, has a simple structure, less maintenance cost, low operating noise and is capable of starting at low wind speed. However, Savonius turbines have some drawbacks, such as relatively low power coefficient and low rotational velocity. Each blade absorbs power for part of the cycle only. The rear shape of the blades requires special consideration to move against the wind direction. Although there are some disadvantages, Savonius turbines are best suited for rooftop energy-harvesting systems. Grant and Kelly⁶ experimented with a turbine of 0.5 m diameter mounted on a rooftop with a duct and found it to be suitable for micro-grid power generation. Small-scale wind turbines (SSWTs) are capable of producing power less than 20 kW. Performance of a wind turbine is measured in terms of power coefficient C_p and/or moment coefficient C_m . Grant and Kelly⁶ reported a C_p value of 0.3 and suggested the need for further studies.

Vast literature on Savonius turbines is available. Experimental studies by Savonius showed maximum C_p as 0.31, while the prototype maximum conversion efficiency was reported to be 0.37. Shankar⁷ carried out an experimental study to determine the effects of blade geometry and wind speed on the Savonius-type turbine and studied the performance characteristics at high wind speed. Blackwell *et al.*⁸ conducted experiments with the Savonius turbine placed inside a wind tunnel by varying parameters such as number of buckets, free stream velocity, rotor height and bucket gap width ratio. The results showed that the fluctuation in static torque was high in

*For correspondence. (e-mail: sjv@iiitdm.ac.in)

the case of rotor with two buckets compared to the three-bucket arrangement. Further, two-blade rotor requires less material for construction. Performance of the rotor was found to increase with Reynolds number (Re) and aspect ratio. The performance was found to be better for the two-bucket arrangement with gap width ratio in the range of 0.1 to 0.15. Alexander and Holownia⁹ performed an experimental study of the Savonius turbine by varying the number of blades, gap width ratio, overlap ratio, aspect ratio, addition of extension pieces, end plates and shielding with three different wind tunnels. They found that the efficiency was generally low for low aspect ratio, unshielded rotors without end plates. However, they found maximum C_p of 0.243 at the highest aspect ratio (4.8), which had optimized blade and shielding configuration. Khan¹⁰ conducted an experiment with prototype and scaled models by varying rotor shape, overlap between rotor blades and the separation gap between rotor blades at three different wind velocities inside the wind tunnel. The results were found to be affected by the interference due to wind tunnel wall. However, the results can be used to optimize rotor designs. The results showed that the optimum overlap between blades depends on the shape of the rotor. Overlap was expressed as percentage of the projected width. The optimum overlap was 16% of width of conventional rotors, whereas it was 30% for the modified rotor¹⁰. Inclusion of the separation gap between the rotor blades caused an adverse effect on the performance. The peak efficiency was constant for all rotor configurations at different wind velocities; full-scale prototype showed maximum C_p of 0.32 and maximum tip speed ratio of 1.55. The prototype showed the ability to generate power even at low wind speed (6.5 kmph). Sivasegaram¹¹ conducted an experimental study by varying the parameters such as number of blades, blade angle, blade location and angle of setting of the blade based on performance criteria, viz. turbine efficiency and the efficiency normalized with respect to blade area. The scaled-down model of the turbine with two-blade rotor showed maximum efficiency with 180° blade angle, whereas based on blade area the maximum efficiency of turbine was 150° blade angle. Ushiyama *et al.*¹² conducted an experimental study of the Savonius turbine placed in a wind tunnel by varying seven parameters, viz. aspect ratio, overlap and gap between rotor, profile of the bucket cross-section, number of buckets, end-plate effects and the influence of stack of buckets. They concluded that within their range of study, large aspect ratio of 4.29 gave maximum torque and power characteristics; the overlap ratio recommended was 20% and 30%, increase in gap ratio reduced the torque coefficient. At low tip speed ratio with 10% to 30% overlap ratio, Bach-type rotors were found to be superior to Savonius rotors. Double-stacked two-blade rotor with end plates showed better results. Modi and Fernando¹³ conducted an experimental study employing a semi-empirical approach to predict the rotor performance using measured

stationary blade pressure. They suggested an aspect ratio of 0.77 and blade angle 135° with no overlapping and gap width ratio. Peak power coefficient was found to be 0.32 at a tip speed ratio of 0.79. The authors suggested considering blockage factor while conducting experiments in the wind tunnel¹³. Fujisawa and Gotoh¹⁴ measured experimentally the pressure distribution on the blade surfaces with rotation at various tip speed ratios and without rotation at various rotor angles. They evaluated torque and power performances by integrating the pressure, which was found to be in good agreement with direct torque measurement. The change in drag coefficient at low tip speed ratios showed the influence of separation control effect on the convex side of the advancing blade, while the side force coefficient remained zero at all tip speed ratios. Saha and Rajkumar¹⁵ experimentally found better performance of twisted blades over conventional blades. They reported that the twisted blades showed smooth running, higher efficiency and good self-starting capacity than the conventional rotor. The twist in the blade provides a longer moment arm. Hence the net positive drag increases and energy capture in the lower part of the blade decreases, which means the net positive torque decreases. By introducing and increasing the twist angle of rotor blades, the performance of the Savonius rotor can be improved. A twist angle of 15° was suggested to operate the turbine at low wind speed. Two-stage rotor was recommended to eliminate stalling problem and found to be efficient. The authors concluded that the twisted turbine had 22% improved performance¹⁵. Akwa *et al.*¹⁶ numerically studied the effect of overlap ratio and recommended a value of 0.15. The overlap ratio increases the performance due to effective reorientation of airflow direction. Ferrari *et al.*¹⁷ conducted a CFD study using 2D and 3D computational domains and suggested an aspect ratio of 1.01 for better performance.

Concavity in the advancing blade receives more drag than convexity in the returning blade and thus torque is developed. Researchers have proposed several modifications to the shape of the blade. Ogawa and Yoshida¹⁸ added a deflecting plate just in front of the returning blade aiming to increase the power coefficient. They reported from the experimental results that relative increase in power coefficient was more than 24% compared to the conventional arrangement. Reupke and Probert¹⁹ used the slatted blade technique to conduct an experimental study. The results showed that the performance of the slatted blades was poor compared to the conventional rotor. Altan *et al.*²⁰ introduced curtain arrangement in their experimental study and found improvement by 38.5% compared to conventional arrangement. Kamoji *et al.*²¹ experimentally tested helical rotors with and without a shaft between them. They found that all the helical Savonius rotors had positive coefficient of static torque at lower coefficient of power than those without shaft. Mohamed *et al.*²² numerically introduced obstacle plate

with inclination towards advancing rotor to reduce drag on the returning blade and to increase drag on the advancing blade. The performance was found to increase by 27%. Mohamed *et al.*²³ varied the shape of blades as well as included an obstacle plate, and reported 30% overall improvement. Abraham *et al.*²⁴ proposed vent and capping of vent in the blades and found improvement in performance. Kacprzak *et al.*²⁵ evaluated the performance of Bach, elliptical and conventional-type blade rotors and reported that Bach type performs better than the others. Only at lower tip speed ratio (TSR) did elliptic shape perform better. Nasef²⁶ modified the shape of the conventional turbine at selective locations of the cross-sections and reported better performance. Jeon *et al.*²⁷ reported increase in turbine performance due to increase in area of end plate. Tartuferi *et al.*²⁸ numerically proved that airfoil-type blades result in higher performance of the Savonius wind rotor. Sharma and Sharma²⁹ numerically studied the performance of Savonius turbine by introducing multiple quarter blades and found an improvement in coefficient of power ranging between 8.89% and 13.69%. Sanusi *et al.*³⁰ reported that the combined elliptical and conventional blades improve C_p up to 11% at $TSR = 0.79$. Alom and Saha³¹ reported that blades with vented rotors had 8.08% more power coefficient than non-vented blades with elliptical profile. Tian *et al.*³² modified the thickness of the blades and reported 4.41% higher C_p . Kerikous and Thévenin³³ modified the blade shape to divert flow on the advancing blade and reported 15% increase in C_p at $TSR = 1.2$. Glass and Levermore³⁴ conducted an experimental study under real weather conditions over a period of one year for five different micro turbines. They reported 40 kWh of actual power generation against the theoretical calculation of 201 kWh annually. Li *et al.*³⁵ reported that the micro wind turbine could be operated at an average wind speed of 2.7 m/s, and found maximum annual output of 82.1 kWh. Kakran and Chanana³⁶ conducted experiments using the wind turbine in a residential community and reported significant reduction in the cost of electricity consumption. Alli and Jayavel³⁷ conducted a numerical study on the performance of Savonius VAWT with and without omni-directional guide vane. It can be observed from the literature that there are many possible ways to improve the performance of Savonius turbine. Even a small improvement in the performance yields a large gain in power over a long period. From an application point of

view, Savonius turbine is more suitable to be mounted on the rooftops of buildings for power generation, where low to moderate wind speed is available. The present study focuses on the methods to improve the performance of Savonius-type VAWTs.

We did a literature review of both experimental and numerical studies carried out on Savonius turbines. Table 1 lists the key design variables that were found to give maximum C_p .

A numerical analysis was done on the performance parameters of the Savonius turbine. Capped vents were introduced in the conventional Savonius blade exactly at the mid-location. Besides, modifications in the vent shape were carried out. Vents of four different configurations namely outer converging, outer diverging, inner converging, and inner diverging were analysed and their effects on the performance were studied systematically.

Capped vents were mounted on the blades of the conventional rotors with the expectation of reducing drag on the returning blades. The shapes of the capped vents were also changed and performance improvement was studied. Although reduction in drag on the returning blade was observed, the results showed reduction in overall performance.

Problem description

The present two-dimensional numerical study on blade modification is a continuation of studies reported by Abraham *et al.*²⁴ and Alom and Saha³¹. The maximum theoretical percentage of power that can be extracted from an ideal wind stream is 59.26. This is referred to as the Betz's limit, formulated in 1919. Within this given limit, the present study was aimed to identify

Table 1. Summary of key design variables from the literature review

Turbine type	Savonius S-shaped
Number of blades	2
Gap width ratio (e/d)	0.15
Overlap ratio (s/d)	0
Blade arc angle	180°

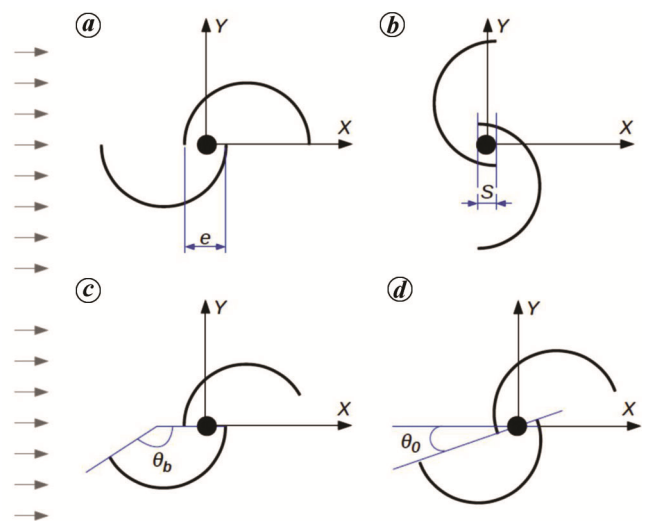


Figure 1. Schematic representation of Savonius-type vertical axis wind turbine with two-blade rotor: *a*, gap width; *b*, overlap; *c*, blade arc angle; *d*, measure of rotation angle.

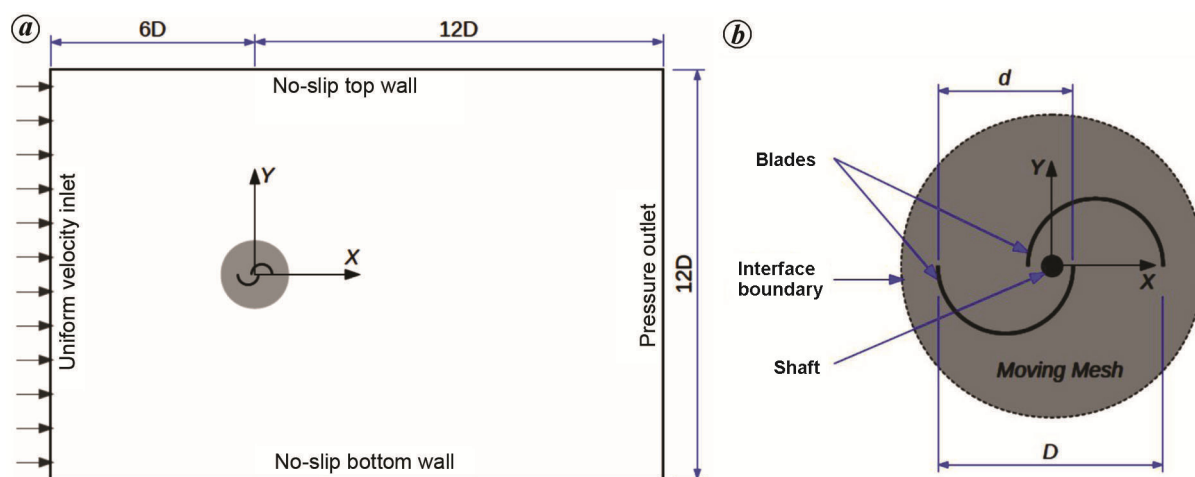


Figure 2. Computational domain. *a*, Location of rotor within the domain. *b*, Enlarged view of the rotor.

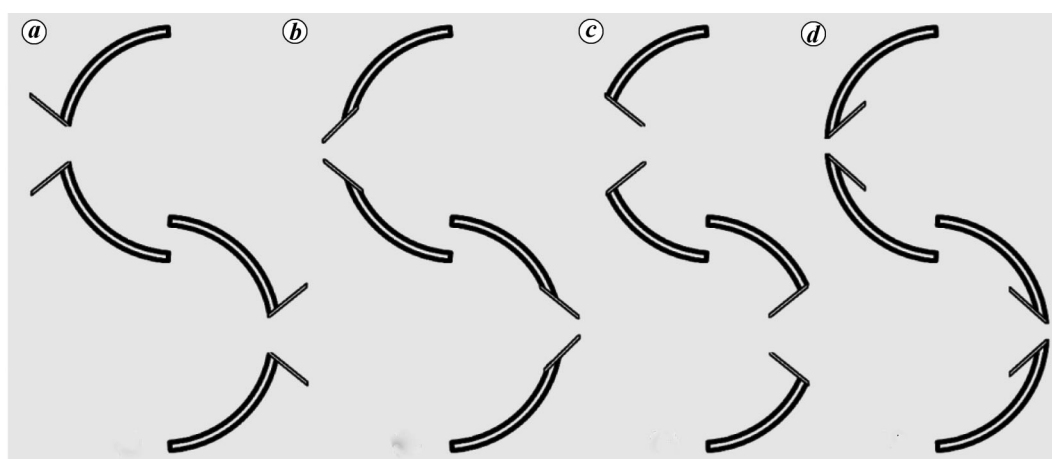


Figure 3. Schematic representation of the blades with modifications. *a*, Outer converging (OC); *b*, Outer diverging (OD); *c*, Inner converging (IC); *d*, Inner diverging (ID).

the possible configuration to provide the best performance.

First, the effect of various design parameters on the performance of Savonius rotor was examined. Although design parameters have been independently studied by various researchers, in the present study all important design parameters with respect to small VAWTs have been evaluated in detail. Secondly, the blade of the conventional rotor was modified with a vent fitted at the mid-location to reduce drag on the returning blade.

Model description and computational domain

Conventional Savonius turbine consists of semi-circular blades mounted on a central shaft. The effect of the shaft on flow characteristics is not considered in the present numerical study. Air is considered as a working fluid. Figure 1 shows the rotor blades. The thickness of the blades is 2 mm. The flow and associated gradients along

height of the rotor are negligible; therefore two-dimensional numerical study was conducted with respect to the plane perpendicular to the axis of the turbine. Figure 1 *a–d* shows the gap width, overlap, blade arc angle and measure of rotation angle respectively. The two-dimensional computational domain consists of a rotor of diameter D , with side confinements (Figure 2). All the length scales are non-dimensionalized with respect to rotor diameter. The effect of rotor geometric parameters, viz. gap width ratio, overlap ratio and blade arc angle on the performance was studied. Figure 3 shows the modified blades; modifications are named with reference to the returning blade.

Governing equation and solution methodology

The incompressible two-dimensional Navier–Stokes equations were obtained from integral form of the general convection–diffusion transport equation equipped with a

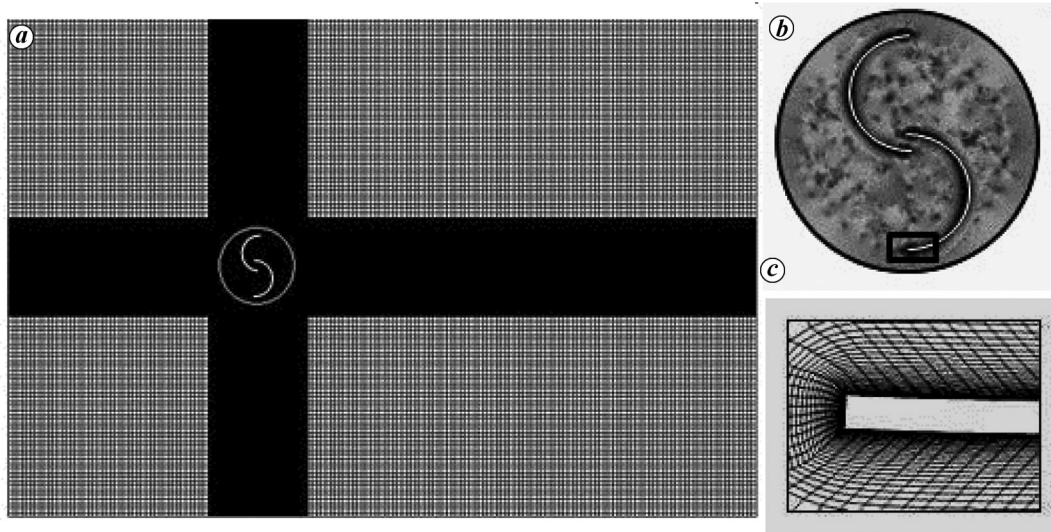


Figure 4. Meshing model: *a*, overall domain; *b*, rotating domain; *c*, near the blade.

Table 2. Summary of grid independence study

Number of elements	Averaged (cm)	Deviation (%)
74,146	0.2635	–
92,162	0.2828	7.32
107,250	0.2715	3.99
130,905	0.2765	1.84
145,104	0.2754	0.39

source term (eq. (1)). By setting the transport property ϕ equal to 1, u and v the respective mass and momentum equations were obtained. The diffusion coefficients, Γ_ϕ is assigned as μ . The source terms, S_ϕ is assigned either $\partial p/\partial x$ or $\partial p/\partial y$

$$\frac{\partial}{\partial t} \int_V \rho \phi \, dV + \int_S [\rho \bar{u} \phi - \Gamma_\phi \nabla \phi] \, d\vec{S} = \int_V S_\phi \, dV. \quad (1)$$

The governing equations are elliptic in nature and so the boundary conditions are specified over the entire boundary of the solution domain at all times. The boundary conditions were no-slip for blade surface and side-confining walls. Symmetry for side walls, uniform velocity ($u = 7$ m/s) at the inlet and pressure outlet at the exit were used. The rotor was housed in a rotating domain of $1.2D$ diameter, which was surrounded by a stationary rectangular domain. An interface was created between the stationary and rotating domains. The rotating domain was imposed with angular speed calculated from the required TSR. The SST $K-\omega$ turbulence model was used to simulate turbulent flow field with flow separation over the surface of the rotor. For the present computation 5% turbulence intensity has been imposed at the inlet with $y^+ < 1$. A finite volume-based software, ANSYS-Fluent

was used for numerical computations of the governing equations. Semi-implicit discretization for pressure-linked equations was used to solve the discretized flow equations. Second-order quadratic upwind scheme for convection kinematics was used for discretization of convective fluxes. Computations were carried out for 10 s with time step size of 0.005 s.

Meshing and grid independence study

Unstructured mesh was generated for the interior rotating domain and structured mesh generated in the outer rectangular domain using ANSYS-meshing tool. Figure 4 *a* shows the generated mesh, while Figure 4 *b* shows the rotor along with the rotating domain. Figure 4 *c* depicts an enlarged view of the mesh near the blade tip. Grid independence study was carried out to obtain accurate results within a reasonable time. The parameter C_m was used to study the effect of mesh size. Table 2 shows the results. For further studies, optimum mesh size was identified as 130,905.

Results and discussion

The power coefficient (C_p) indicates the conversion efficiency of the turbine. It is the ratio of shaft power (P_s) and wind power (P_w) (eq. (2)). P_s is calculated from brake torque (T_s) and angular velocity (ω) of the turbine. For an airstream flowing through a cross-section area A , the mass flow rate is (ρAu) , and kinetic energy of air $(1/2 \rho u^2)$ P_w is calculated from eq. (4).

$$C_p = \frac{P_s}{P_w} = \frac{T_s \omega}{\frac{1}{2} \rho A u^3}, \quad (2)$$

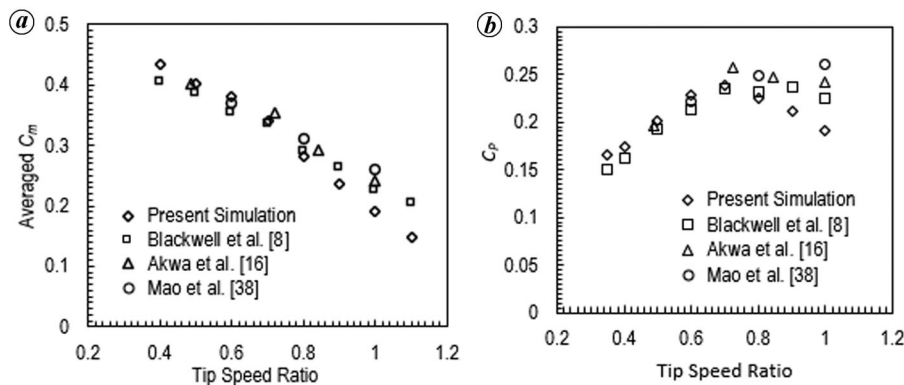


Figure 5. Effect of tip speed ratio (TSR) on (a) C_{m-avg} and (b) C_p .

$$P_w = \rho Au \times \frac{1}{2} u^2 = \frac{1}{2} \rho Au^3, \tag{3}$$

$$C_m = \frac{T_s}{T_w} = \frac{T_s}{\frac{1}{2} \rho Au^2 R}, \tag{4}$$

$$T_w = \frac{1}{2} \rho u^2 \times AR = \frac{1}{2} \rho Au^2 R, \tag{5}$$

$$\lambda = \frac{C_p}{C_s} = \frac{R\omega}{u}. \tag{6}$$

Torque coefficient or coefficient of moment (C_m) as given in eq. (4) is the dimensionless parameter, which relates shaft torque (T_s) and wind torque (T_w). Wind torque is calculated using eq. (5). Tip speed ratio, λ is defined as the ratio of linear velocity at the tip to the free stream velocity. C_m has been averaged from the available values for two complete revolutions of the rotor. The study was conducted for various TSRs. The results were validated using those from other studies^{8,16,38}. The present results match well with those in the literature (Figure 5 a). Figure 5 b shows the effect of TSR on C_p . Maximum C_p is observed at TSR = 0.8 (approx.). Subsequent numerical studies were conducted for TSR = 0.8. The simulations were carried out considering fully turbulent flow²⁴. At higher-tip TSR (> 0.8), under turbulent condition, the flow characteristics are complicated near the blade tip, which is fast moving. Though the average value of C_m has been calculated for a complete rotation of the rotor, at higher TSR the results deviate more due to the complicated flow characteristics.

In the present study, two-dimensional simulations has been carried out. The end effect of the rotor blades are suppressed due to the two-dimensional study. However, for comparison of overall performance, the two-dimensional assumption is acceptable. The inlet turbulence intensity is highly uncertain due to environmental conditions. In the present study, a suitable value was chosen from the litera-

ture. Moreover, the same value was used for all the cases, so that the sole effect of change in design parameter could be captured.

Effect of number of blades

The effect of number of blades on rotor performance was studied. The number of blades considered for the study were 2, 3 and 4 and accordingly, the different cases were designated as 2-B, 3-B and 4-B respectively. Moment coefficient and drag coefficient were computed for each blade and for the overall rotor. From the study, it was observed that the 2-B rotor system showed more fluctuation in torque compared to 3-B and 4-B rotor systems. Increasing the number of blades reduced the torque fluctuation and power generation was smoother. Table 3 summarizes the effect of number of blades used. Figures 6–8 show variation in moment and drag coefficients for one complete revolution. Though the torque fluctuation was more, the rotor system with 2-B arrangement was observed to give better performance (Figure 9). Figure 10 shows pressure and velocity distributions with 2-B, 3-B and 4-B configurations for TSR = 0.8. As the number of blades increases, the time-period available for the advancing blade to face the wind in reduced. Therefore, the 2-B configuration has the ability to extract maximum energy than the 3-B and 4-B configurations. In the downstream, the vortices formation and its size show unsteadiness. From the pressure distribution, it can be concluded that in the 2-B configuration, the advancing blade is subjected to higher pressure for a longer time. From the velocity distribution it can be observed that low velocity region is present in the downstream, which is an indication of higher pressure. This phenomenon increases with the number of blades.

Static torque variation

The static torque due to wind force on stationary Savonius rotor was studied. The net torque is the difference in

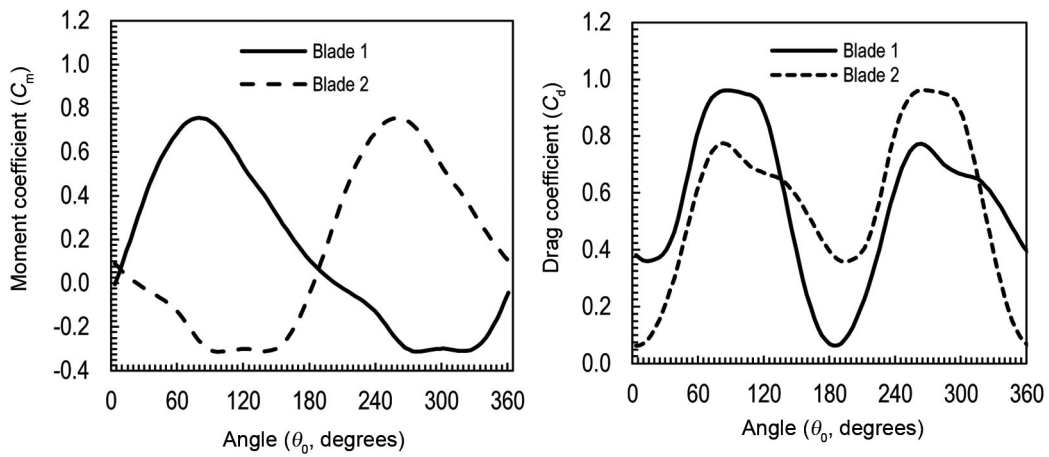


Figure 6. Variation of C_m and C_d for one rotation of the rotor with two blades.

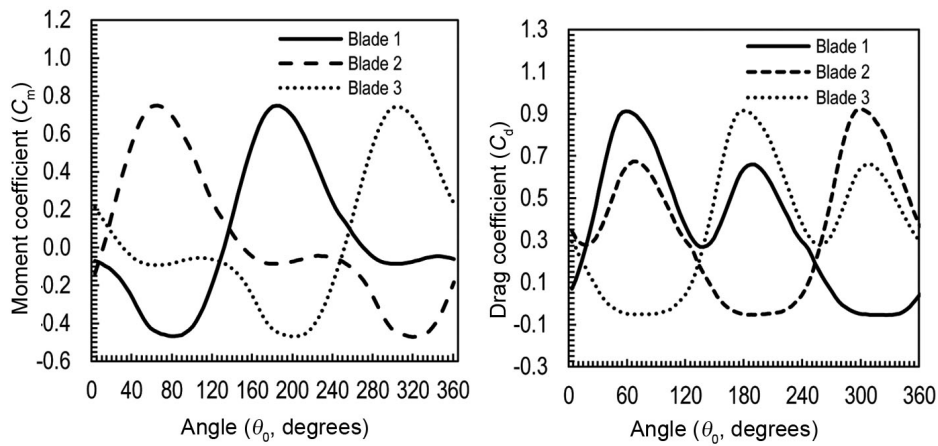


Figure 7. Variation of C_m and C_d for one rotation of the rotor with three blades.

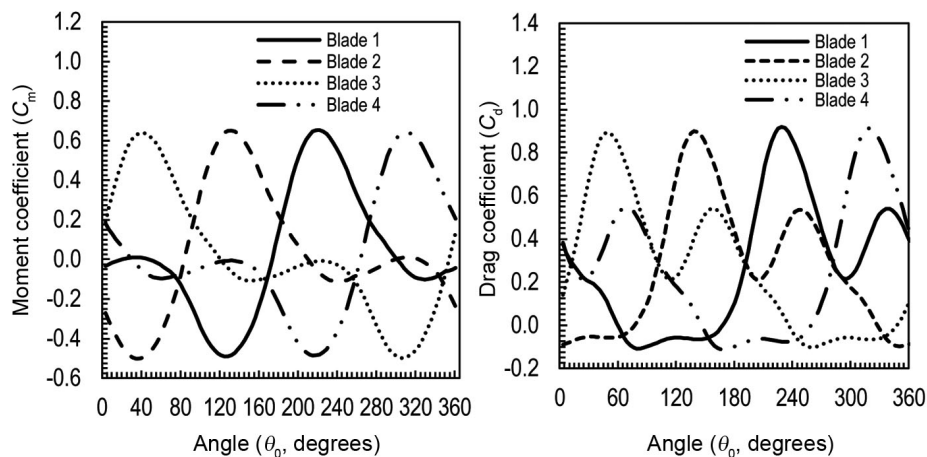


Figure 8. Variation of C_m and C_d for one rotation of the rotor with four blades.

drag between advancing and returning blades of the rotor. The net torque changes with angular position of the rotor (i.e. θ_0). Figure 11 shows the static torque variation with

respect to θ_0 . The shape of the torque – θ_0 curve and the peak static torque depend on parameters such as number of blades, blade geometry and overlap ratio. The study

Table 3. Effect of number of blades on rotor performance

Rotor performance	Number of blades	Blades considered	Maximum	Minimum	Average
Drag coefficient (C_d)	2-B	Individual	0.961	0.063	0.561
		Overall	1.736	0.431	1.120
	3-B	Individual	0.920	-0.052	0.368
		Overall	1.528	0.649	1.096
	4-B	Individual	0.911	-0.065	0.271
		Overall	1.353	0.777	1.054
Moment coefficient (C_m)	2-B	Individual	0.756	-0.313	0.137
		Overall	0.559	-0.013	0.285
	3-B	Individual	0.751	-0.469	0.048
		Overall	0.246	-0.024	0.123
	4-B	Individual	0.653	-0.502	0.020
		Overall	0.129	0.032	0.076
Static torque coefficient (C_m^*)	2-B	Overall	0.979	0.008	0.576
	3-B	Overall	0.680	0.164	0.385
	4-B	Overall	0.307	0.064	0.204

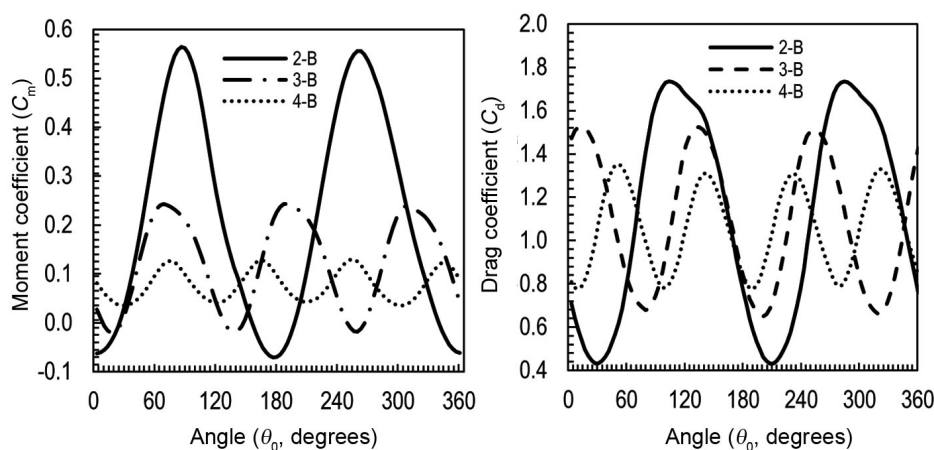


Figure 9. Variation of net C_m and C_d for one rotation of the rotors with two (2-B), three (3-B) and four (4-B) blades.

has been conducted for rotors with 2-B, 3-B and 4-B. Figure 11 also shows the 2-B rotor and associated torque variations. Close to $\theta_0 = 180^\circ$ and 360° , both blades of the 2-B rotor develop very small or almost zero torque. This indicates the inability of the rotor to self-start, when wind velocity is in these particular directions. However, while the rotor rotates, the maximum static torque felt by it is at angular positions of 80° and 260° , which are highly favourable for self-starting. On the other hand, the 3-B and 4-B rotors develop positive torque for all values of θ_0 , therefore rotors with three or more blades can self-start with any wind direction.

As shown in Figure 11, the average torque developed by the rotor decreases with increasing number of blades. Drag, moment and static torque coefficients were calculated (Table 3). The average moment coefficient was found to decrease with the increasing number of blades. The values of moment coefficient for 2-B, 3-B and 4-B rotors were 0.28, 0.123 and 0.076 respectively. Increase

in the number of blades lowered the value of overall C_d as well.

Effect of gap width ratio and overlap ratio

Figure 12 shows the effects of gap width ratio (e/d) and overlap ratio (S/d) on average moment coefficient (C_m) for $TSR = 0.8$. In the present study, the effect of gap width ratio in the range $0 \leq e/d \leq 0.2$ was evaluated. When $e/d > 0$, the advancing blade redirects a part of the flow inside the returning rotor, thereby increasing the net positive drag. On the other hand, for higher e/d ratio, the overall performance decreases. This is due to considerable decrease in the available frontal area of the advancing rotor. It was observed that the rotor with gap width ratio of 0.1–0.2 performed better than the other configurations. Therefore, it is preferable to use $e/d = 0.15$. Overlap between rotors leads to unfavourable flow characteristics, thereby decreasing rotor performance.

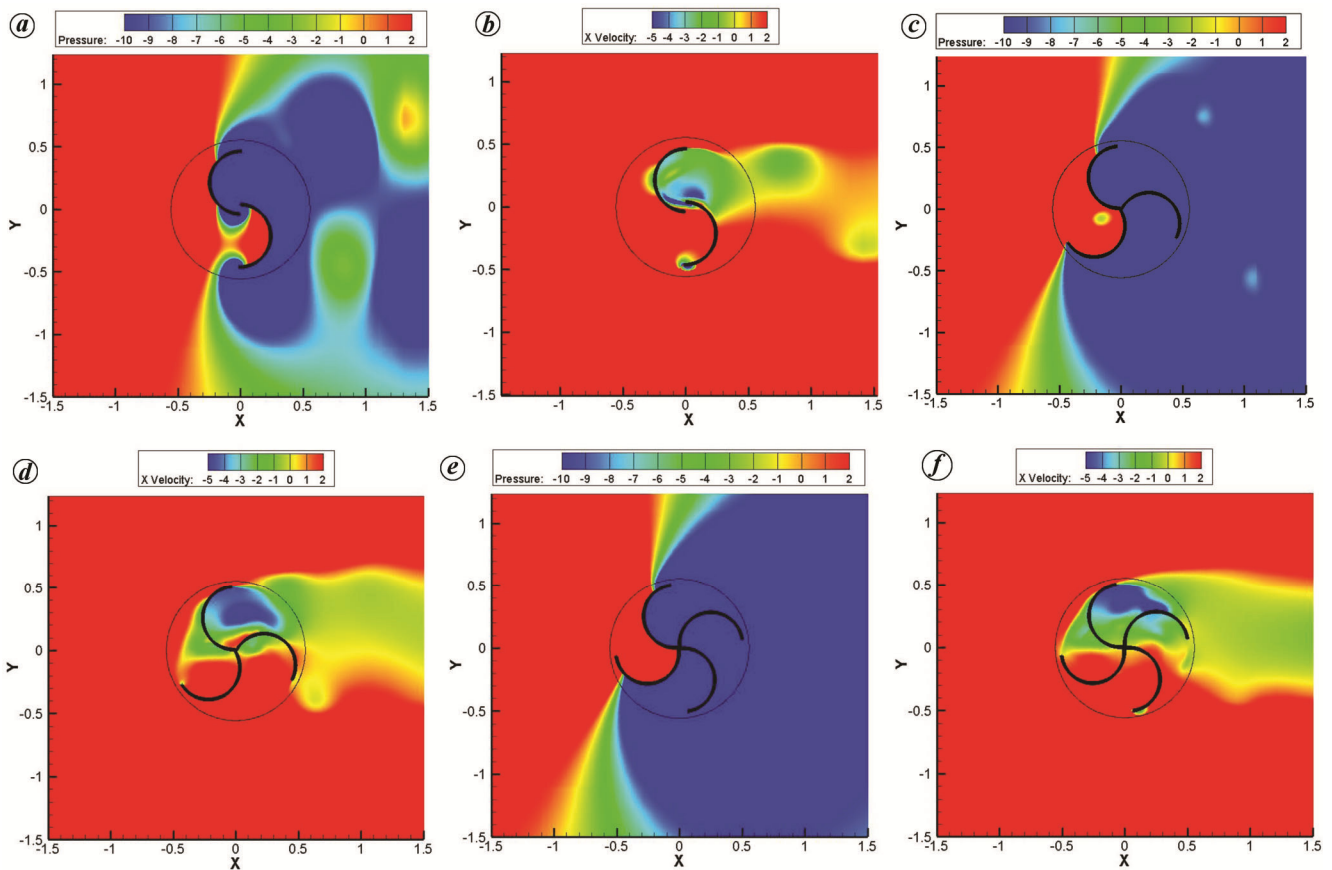


Figure 10. Pressure and velocity distribution for various number of blades. (Left) Pressure distribution and (right) Velocity distribution: *a, b*, with 2-B; *c, d*, with 3-B; *e, f*, with 4-B.

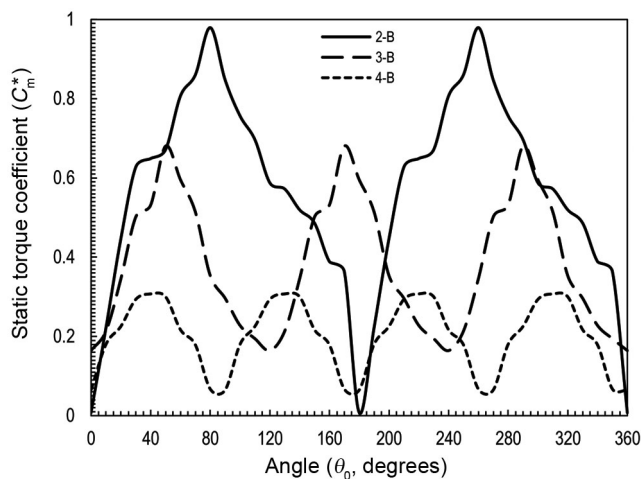


Figure 11. Comparison of static torque coefficient over one complete rotation of the rotor.

Effect of blade arc angle

Blade arc angle affects the performance of the rotor. Concavity in advancing blade helps in gaining energy

from the wind; the blade arc angle determines the level of concavity. The study was carried out at TSR of 0.8 by varying the blade arc angle starting from 150° with 10° increments up to 210°. The results are shown in Figure 13, where the blade arc angle with 180° (semi-circular blade) gives maximum performance.

Blades with modification

Let us discuss the variation of C_m and C_d over one complete revolution of the rotor. Either we can modify the front shape of the rotor to get more drag when it acts as an advancing blade, or modify the rear shape to reduce drag while it acts as a returning blade. Modifying both front and rear shape of the rotor could improve the net drag effectively. Figure 3 shows the schematic of the modifications. The objective is to reduce drag on the returning blade. During one complete revolution, at the time of advancing action the diffuser effect will be felt by the blade. When the same blade is subjected to returning action, nozzle effect is experienced by the blade as shown in Figure 3*a*. Thereby the net drag is expected to increase. Later, the vent orientations are reversed in the

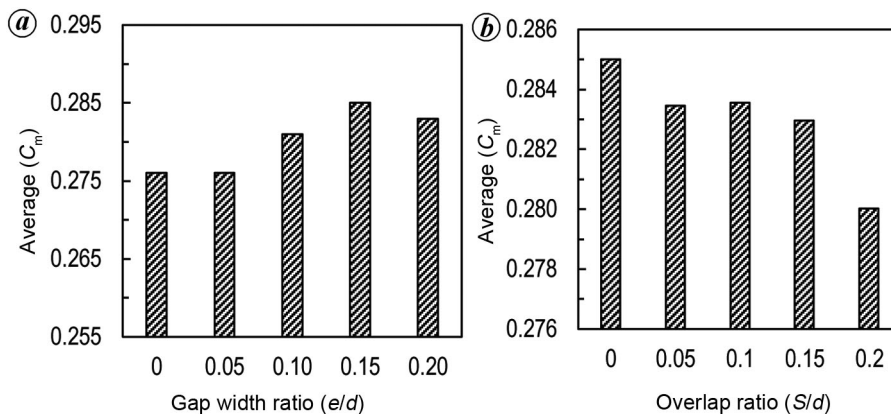


Figure 12. Effect of (a) gap width ratio and (b) overlap ratio on C_m .

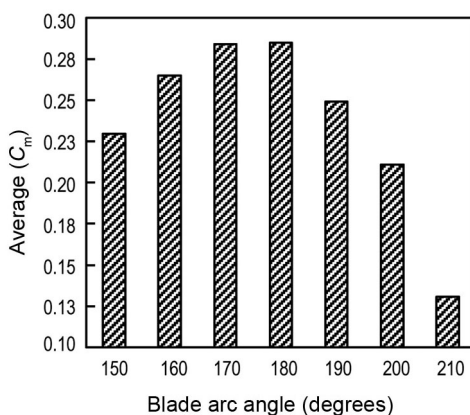


Figure 13. Effect of blade arc angle on C_m .

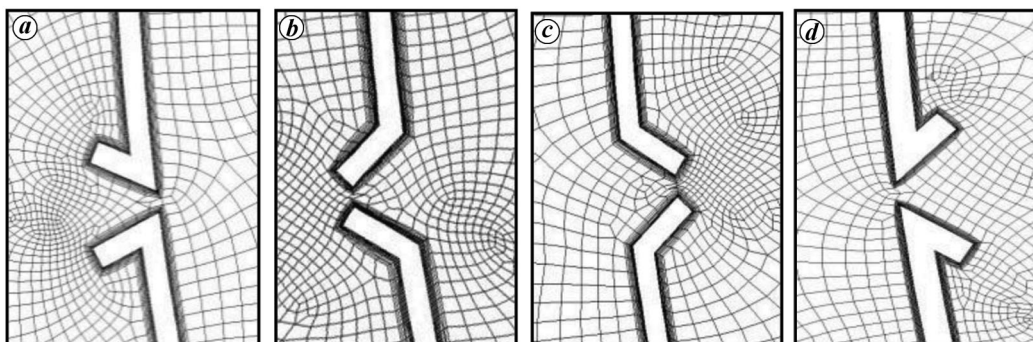


Figure 14. Mesh near the capped vents. a, Outer converging (OC); b, Outer diverging (OD); c, Inner converging (IC); d, Inner diverging (ID).

blade and the effects studied. Figure 14 shows meshing near the capped vents while Figure 15 shows results. When compared to conventional rotor, the reductions in C_m for inner diverging (ID) and outer diverging (OD) are 5.7% and 7.6% respectively. For inner converging (IC) and outer converging (OC), the reductions in C_m are 6.9% and 8.4% respectively. As discussed above, each blade plays the role of advancing action and returning action. When the blade arc angle is 180°, during the advancing role, the blade frontal area open to the wind is larger.

Therefore, it captures more energy from the wind. On the other hand, during the returning role, the blade effectively deflects air to the other blade which is advancing. Thus the blade with 180° arc angle performs better. Output of the blades with modifications is reduced due to the following reasons. When the blade arc angle are reduced or increased, the frontal area and the wind deflection towards the advancing blade are affected. Blades with capped vents are subjected to reduction in effective frontal area.

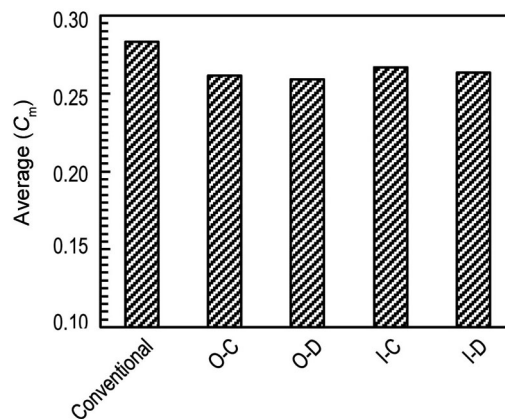


Figure 15. Averaged C_m for different shapes.

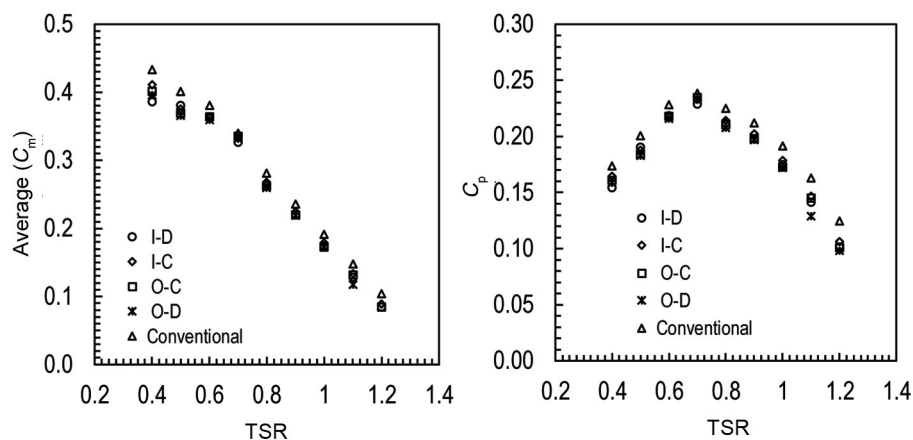


Figure 16. Effect of TSR on average C_m and C_p .

Figure 16 compares the average C_m and C_p with respect to TSR for the four cases, viz. IC, OC, ID and OD. The results show that the modification in the form of vent leads to reduction in power conversion.

At lower TSR, there is difference in power conversion due to different types of capped vents. However, at higher TSR, the performance of all capped vents is more or less the same. Also, at higher TSR, the presence of capped vents reduces the form drag on the returning blades.

Conclusion

In addition to a thorough review of the literature, two-dimensional unsteady numerical analysis was carried out to study the performance of Savonius turbine due to the effect of various parameters such as number of blades, overlap ratio, gap width ratio, blade arc angle and modification in the rotor blades. From the study, the following conclusions are made.

(1) The performance of 2-B, 3-B and 4-B rotors was evaluated and it was found that increase in the number of blades reduced the moment fluctuation, therefore resulting

in smooth operation and less vibration. On the other hand, for a given TSR, increase in the number of blades led to reduction in the average C_m . Although 2-B rotor develops vibrations due to fluctuating moment, from a performance point of view, the 2-B rotor is preferable. Moreover, strong structural support can withstand vibration.

(2) The study on static torque variation showed the ability of the rotor to self-start. The 2-B rotor showed larger starting torque for some wind directions. However, for some others, the starting torque in the case of 2-B rotor was zero. Two-stage rotor assembly can eliminate this drawback.

(3) Geometric parameters of blade such as arc angle (150° – 210°), gap width ratio, overlap ratio and modification in the blade were studied. The results showed that the performance of the rotors with blade arc angle of 180° and gap width ratio of 0.15 was preferable. However, overlap and capped vent in the present form were not preferable.

1. Born, F. J. *et al.*, On the integration of renewable energy systems within the built environment. *Build. Serv. Eng. Res. Technol.*, 2001, 22(1), 3–13.

2. <https://windexchange.energy.gov/small-wind-guidebook> (accessed on 1 June 2019).
3. Johannes, S. S. (inventor), Rotor adapted to be driven by wind or flowing water. United States patent US 1697574, 1929.
4. Savonius, S. J., The S-rotor and its applications. *Mech. Eng.*, 1931, **53**(5), 333–338.
5. Savonius, S. J., The wing-rotor in theory and practice. Omnia-Mikrofilm-Technik, 1981.
6. Grant, A. and Kelly, N., A ducted wind turbine model for building simulation. *Build. Serv. Eng. Res. Technol.*, 2004, **25**(4), 339–349.
7. Shankar, P. N., The effects of geometry and Reynolds number on Savonius type rotors. NAL Memorandum AE-TM-3-76, National Aerospace Laboratory, Bengaluru, 1976.
8. Blackwell, B. F., Sheldahl, R. F. and Feltz, L. V., Wind tunnel performance data for two-and three-bucket Savonius rotors. Sandia Laboratories, Springfield, VA, USA, 1977.
9. Alexander, A. J. and Holownia, B. P., Wind tunnel tests on a Savonius rotor. *J. Wind Eng. Ind. Aerodyn.*, 1978, **3**(4), 343–351.
10. Khan, M. H., Model and prototype performance characteristics of Savonius rotor windmill. *Wind Eng.*, 1978, **2**(2), 75–85.
11. Sivasegaram, S., An experimental investigation of a class of resistance-type, direction-independent wind turbines. *Energy*, 1978, **3**(1), 23–30.
12. Ushiyama, I., Nagai, H. and Shinoda, J., Experimentally determining the optimum design configuration for Savonius rotors. *Bull. JSME*, 1986, **29**(258), 4130–4138.
13. Modi, V. J. and Fernando, M. S., On the performance of the Savonius wind turbine. *J. Solar Energy Eng.*, 1989, **111**(1), 71–81.
14. Fujisawa, N. and Gotoh, F., Experimental study on the aerodynamic performance of a Savonius rotor. *J. Solar Energy Eng.*, 1994, **116**(3), 148–152.
15. Saha, U. K. and Rajkumar, M. J., On the performance analysis of Savonius rotor with twisted blades. *Renew. Energy*, 2006, **31**(11), 1776–1788.
16. Akwa, J. V., da Silva Júnior, G. A. and Petry, A. P., Discussion on the verification of the overlap ratio influence on performance coefficients of a Savonius wind rotor using computational fluid dynamics. *Renew. Energy*, 2012, **38**(1), 141–149.
17. Ferrari, G., Federici, D., Schito, P., Inzoli, F. and Mereu, R., CFD study of Savonius wind turbine: 3D model validation and parametric analysis. *Renew. Energy*, 2017, **105**, 722–734.
18. Ogawa, T. and Yoshida, H., The effects of a deflecting plate and rotor end plates on performances of Savonius-type wind turbine. *Bull. JSME*, 1986, **29**(253), 2115–2121.
19. Reupke, P. and Probert, S. D., Slatted-blade Savonius wind-rotors. *Appl. Energy*, 1991, **40**(1), 65–75.
20. Altan, B. D., Atılgan, M. and Özdamar, A., An experimental study on improvement of a Savonius rotor performance with curtaining. *Exp. Therm. Fluid Sci.*, 2008, **32**(8), 1673–1678.
21. Kamoji, M. A., Kedare, S. B. and Prabhu, S. V., Performance tests on helical Savonius rotors. *Renew. Energy*, 2009, **34**(3), 521–529.
22. Mohamed, M. H., Janiga, G., Pap, E. and Thévenin, D., Optimization of Savonius turbines using an obstacle shielding the returning blade. *Renew. Energy*, 2010, **35**(11), 2618–2626.
23. Mohamed, M. H., Janiga, G., Pap, E. and Thévenin, D., Optimal blade shape of a modified Savonius turbine using an obstacle shielding the returning blade. *Energy Convers. Manage.*, 2011, **52**(1), 236–242.
24. Abraham, J. P., Plourde, B. D., Mowry, G. S., Minkowycz, W. J., and Sparrow, E. M., Summary of Savonius wind turbine development and future applications for small-scale power generation. *J. Renew. Sustainable Energy*, 2012, **4**(4), 042703.
25. Kacprzak, K., Liskiewicz, G. and Sobczak, K., Numerical investigation of conventional and modified Savonius wind turbines. *Renew. Energy*, 2013, **60**, 578–585.
26. Nasef, M. H., A new design of Savonius wind turbine: numerical study. *CFD Lett.*, 2015, **6**(4), 144–158.
27. Jeon, K. S., Jeong, J. I., Pan, J. K. and Ryu, K. W., Effects of end plates with various shapes and sizes on helical Savonius wind turbines. *Renew. Energy*, 2015, **79**, 167–176.
28. Tartuferi, M., D'Alessandro, V., Montelpare, S. and Ricci, R., Enhancement of Savonius wind rotor aerodynamic performance: a computational study of new blade shapes and curtain systems. *Energy*, 2015, **79**, 371–384.
29. Sharma, S. and Sharma, R. K., Performance improvement of Savonius rotor using multiple quarter blades – a CFD investigation. *Energy Convers. Manage.*, 2016, **27**, 43–54.
30. Sanusi, A., Soeparman, S., Wahyudi, S. and Yuliati, L., Experimental study of combined blade Savonius wind turbine. *Int. J. Renew. Energy Res.*, 2016, **6**(2), 614–619.
31. Alom, N. and Saha, U. K., Influence of blade profiles on Savonius rotor performance: numerical simulation and experimental validation. *Energy Convers. Manage.*, 2019, **186**, 267–277.
32. Tian, W., Mao, Z., Zhang, B. and Li, Y., Shape optimization of a Savonius wind rotor with different convex and concave sides. *Renew. Energy*, 2018, **117**, 287–299.
33. Kerikous, E. and Thévenin, D., Optimal shape of thick blades for a hydraulic Savonius turbine. *Renew. Energy*, 2019, **134**, 629–638.
34. Glass, A. and Levermore, G., Micro wind turbine performance under real weather conditions in urban environment. *Build. Serv. Eng. Res. Technol.*, 2011, **32**(3), 245–262.
35. Li, D. H., Cheung, K. L., Chan, W. W., Cheng, C. C. and Wong, T. C., An analysis of wind energy potential for micro wind turbine in Hong Kong. *Build. Serv. Eng. Res. Technol.*, 2014, **35**(3), 268–279.
36. Kakran, S. and Chanana, S., An energy scheduling method for multiple users of residential community connected to the grid and wind energy source. *Build. Serv. Eng. Res. Technol.*, 2018, **39**(3), 295–309.
37. Alli, M. S. and Jayavel, S., Numerical study on performance of Savonius-type vertical-axis wind turbine, with and without omnidirectional guide vane. In *Numerical Heat Transfer and Fluid Flow*, Springer, Singapore, 2019, pp. 449–455.
38. Mao, Z. and Tian, W., Effect of the blade arc angle on the performance of a Savonius wind turbine. *Adv. Mech. Eng.*, 2015, **7**(5), 1–10.

Received 9 March 2020; revised accepted 16 September 2020

doi: 10.18520/cs/v119/i12/1927-1938